

## DECHLORINATION OF CHLORINATED METHANES BY FERROUS ION ASSOCIATED WITH VARIOUS IRON OXIDE MINERALS

Rajapaksha Arachchilage Maithreepala and Ruey-An Doong\*

Department of Biomedical Engineering and Environmental Sciences  
National Tsing Hua University  
Hsinchu 300, Taiwan

**Key Words:** Carbon tetrachloride (CT), iron oxides, surface-bound iron species, dechlorination.

### ABSTRACT

The dechlorination of carbon tetrachloride (CT) by Fe(II) ion in the suspensions of crystalline iron oxide minerals including goethite ( $\alpha$ -FeOOH), hematite ( $\alpha$ -Fe<sub>2</sub>O<sub>3</sub>), magnetite (Fe<sub>3</sub>O<sub>4</sub>), and amorphous ferrihydrite (Fe(OH)<sub>3</sub>) was investigated. Experiments were performed using 10 mM iron oxides and 3 mM Fe(II) to form surface-bound iron suspensions at pH 7.2 under anoxic conditions. Ferrous ion can rapidly sorb onto the surface of iron oxides to form surface-bound iron species. The sorption of Fe(II) onto goethite and hematite followed Langmuir isotherm, while Freundlich isotherm was observed in the magnetite and ferrihydrite suspensions. The major product of CT dechlorination in the iron oxide suspensions containing 3 mM ferrous ion was chloroform (CF) and the conversion ratio of CT to CF was in the range 14-74%, depending on the type of iron oxides. In addition, the dechlorination followed pseudo-first-order kinetics, and the rate constants ( $k_{\text{obs}}$ ) for CT dechlorination were 0.38 h<sup>-1</sup> and 0.84 h<sup>-1</sup> in goethite and hematite suspensions, respectively. Whereas the  $k_{\text{obs}}$  was 0.061 h<sup>-1</sup> for magnetite and 0.014 h<sup>-1</sup> for ferrihydrite, which were lower than those in the highly crystalline iron oxide suspensions. However, the normalized surface area rate constants ( $k_{\text{sa}}$ ) followed the order goethite > hematite > magnetite > ferrihydrite. The solution pH values strongly influenced the rate and efficiency of CT dechlorination and both the  $k_{\text{obs}}$  and sorbed Fe(II) concentrations were exponentially increased with increasing pH value within the range of 4-8.5, depicting that the increase in  $k_{\text{obs}}$  is mainly attributed to the increase in the surface-bound Fe(II) concentration at high pH.

### INTRODUCTION

The contamination of groundwater with chlorinated hydrocarbons is a widespread environmental problem. The environmental and health impacts of chlorinated hydrocarbons have prompted investigations regarding to their attenuation in natural environments. Several chlorinated solvents including carbon tetrachloride (CT), chloroform (CF) and tetrachloroethylene (PCE) are rather persistent under aerobic conditions, but they may undergo reductive dehalogenation under reducing environments [1] due to limited oxygen concentration in both pristine and contaminated subsurface environments. Therefore, the understanding of reductive transformation of chlorinated hydrocarbons under iron-reducing environments is essential from the environmental engineering point of view with respect to the remediation of contami-

nated groundwater or soils.

Fe(II) is one of the natural reductants available in various forms including dissolved, mineral bound, and as hosts of Fe(II)-bearing minerals. Laboratory and field studies have focused on the significance of Fe(II) ion in the abiotic reductive transformation of halogenated compounds in soils and groundwaters [2,3]. Fe(II) ion complexes in dissolved forms have been shown to effectively reduce different types of organic compounds such as polyhalogenated methanes, halogenated ethanes and nitroaromatic compounds under anoxic conditions [4-6]. Several studies have reported that the reactivity of Fe(II) ion in the suspensions of Fe(III)-bearing minerals was higher than that of aqueous Fe(II) ion alone [2,3]. The high reactivity of Fe(II) species attached to solid Fe(III) minerals is rationalized within the framework of surface complexation theory [4]. It is generally believed that, dur-

---

\*Corresponding author  
Email: radoong@mx.nthu.edu.tw

ing the contact of Fe(II) ions with the surface of iron oxide minerals, protons on the surface hydroxyl groups are replaced by Fe(OH)<sub>2</sub> to form  $\equiv\text{Fe}^{\text{III}}\text{OFe}^{\text{II}}\text{OH}$ , and the concentration of the species is proportional to the initial rate of reduction reaction [7]. Recent field studies have further demonstrated that surface-bound Fe(II) was the predominant reductant for nitroaromatic compounds even in geochemically complex polluted aquifers [8]. It depicts that surface-bound Fe(II) system may play a pivotal role as a natural mediator in the *in-situ* reduction of contaminants. Also, several environmental factors such as surface area of iron mineral, available Fe(II) concentration in the aqueous solutions, and pH value of the system can influence the reactivity of surface-bound Fe(II) species. The affinity of the surfaces of different Fe(III) minerals for Fe(II) ions might be the most important factor to form reactive surface Fe(II) sites and should be investigated.

Goethite ( $\alpha$ -FeOOH), hematite ( $\alpha$ -Fe<sub>2</sub>O<sub>3</sub>), magnetite (Fe<sub>3</sub>O<sub>4</sub>), and amorphous ferrihydrite (Fe(OH)<sub>3</sub>) are ubiquitous iron oxides in the natural environments [9]. They have different crystalline properties, surface characteristics and mineralogical characteristics with respect to their originalities. Therefore, the Fe(II) ions associated with iron oxide mineral surfaces may show different reactivities toward the reduction of chlorinated compounds. The objectives of this study were to investigate the dechlorination of CT by Fe(II) ions associated with different iron oxides including goethite, hematite, ferrihydrite and magnetite. CT was selected as the model compound because the reaction of surface-bound iron species is a one-electron transfer process. Moreover, the sorption experiments of Fe(II) onto iron oxides were also performed to verify the reactivity of such systems for the reductive transformation of CT.

## MATERIALS AND METHODS

### 1. Chemicals

All chemicals were used as received without further treatment. CT (> 99.8%, GC grade) and CF (> 99.8%, GC grade) were purchased from Merck Co. (Darmstadt, Germany). N-(2-hydroxyethyl)-piperazine-N'-(2-ethanesulfonic acid (HEPES) (99.5%), 2-(N-morpholino)-ethanesulfonic acid (> 99.5%), FeCl<sub>2</sub>·4H<sub>2</sub>O (99%), and FeCl<sub>3</sub>·6H<sub>2</sub>O (99%) were purchased from Sigma-Aldrich Co. (Milwaukee, WI). Methylene chloride (> 99.8%, GC grade) and ethanol (HPLC grade) were obtained from J. T. Baker (Phillipsburg, NJ).

### 2. Synthesis and Characterization of Iron Oxides

Iron oxides including goethite, hematite, magnetite and ferrihydrite were synthesized following the

procedures of Schwertman and Cornell [10]. After synthesizing the iron oxides in flasks, suspensions of the iron oxides were then transferred into 1-L screw-capped bottles. The bottles were vacuumed (0.66 Pa) for 30 min and then purged with N<sub>2</sub> for 15 min. This process was repeated at least five times while stirring the suspension continuously to maintain the anaerobic conditions. Aliquots of the suspensions were transferred from the sealed bottles into centrifuge tubes using a 100-mL N<sub>2</sub>-purged plastic syringe. The supernatant was removed by centrifugation at 14,000 g for 10 min under N<sub>2</sub> atmosphere. The pellets in the centrifuge tubes were washed five times using deoxygenated deionized water to remove the residual Fe(II) in the solution. After washing, suspensions were transferred anaerobically into a 500-mL serum bottle under a N<sub>2</sub> purge. The bottles were capped with rubber septa followed by vacuuming and N<sub>2</sub> purging for several times before being stored under a N<sub>2</sub> atmosphere.

### 3. Dechlorination Experiments

Batch experiments were conducted using 70-mL serum bottles filled with 50 mL of deoxygenated buffer solution under anaerobic conditions [11,12]. A high purity of N<sub>2</sub> (> 99.9995%) at a flow rate of 42 L min<sup>-1</sup> was used to maintain the anaerobic conditions during the experimental processes. Iron oxides were withdrawn using an N<sub>2</sub>-purged syringe and were delivered into serum bottles to a final concentration of 10 mM. Fe(II) solutions were prepared in deoxygenated buffer solutions in sealed bottles and were introduced into the serum bottles to provide a concentration of 3 mM. HEPES (50 mM) buffer solutions were used to control pH at 7.0±0.1. Bottles were then sealed with Teflon-lined rubber septa and aluminum crimp caps and were incubated in an orbital shaker at 150 rpm and at 25±1 °C in the dark. After 20 h of equilibrium, 25 µL of the CT stock solution dissolved in methanol was delivered into the serum bottle by a gas-tight glass syringe to obtain the final concentration of 20 µM. The total volume of the liquid phase in the serum bottle was maintained at 50 mL, which resulted in a 20-mL headspace left for headspace gas analysis. Parallel experiments were also carried out without the addition of Fe(II). All the experiments were run in duplicate or triplicate.

### 4. Sorption Experiments

In order to understand the sorption behavior of Fe(II) onto the iron oxide minerals, the experimental procedures described in the dechlorination experiments were followed with identical conditions with the exception of CT addition. To study the Fe(II) sorption isotherms onto iron oxides, various volumes of the stock solution of Fe(II) were added to iron oxide suspensions (10 mM) to yield the final concentrations

of 0.05–5 mM. After the addition of Fe(II), bottles were incubated in an orbital shaker (150 rpm) at 25 °C in the dark. After 20 h of equilibrium, 1 mL aliquot was withdrawn using N<sub>2</sub>-purged gastight plastic syringe and 0.5 mL volume was filtered into 1 mL of 0.5 M HCl solution through acidified 0.2 µM filter cartridge (1 cm in diameter). The Fe(II) concentrations in the filtrate was then determined at 562 nm using ferrozine method.

## 5. Analytical Methods

The headspace analytical technique was used to determine the chlorinated hydrocarbons. The concentrations of CT and the byproducts of the test bottles were monitored by withdrawing 50 µL of headspace gas using a 100 µL gas-tight glass syringe. The mixture was then immediately injected into a gas chromatograph (GC) equipped with a flame ionization detector (FID) and an electron capture detector (ECD) (Perkin-Elmer, Autosystem, Norwalk, CT). A 60-m VOCOL fused-silica megabore capillary column (0.545 mm × 3.0 µm, Supelco) was used for separating the chlorinated compounds. The column was connected to FID and ECD simultaneously by a Y-splitter with 40% of the flow (1.85 mL min<sup>-1</sup>) to ECD for better identification and quantification of the chlorinated hydrocarbons. The column temperature was maintained at 90 °C isothermally with N<sub>2</sub> as the carrier gas. Concentrations of chlorinated hydrocarbons in aqueous solutions were then calculated using the external standards by preparing the known concentrations of chlorinated hydrocarbons in aqueous solutions. The relative standard deviation for GC analysis was controlled within 10%.

Concentrations of total HCl extractable Fe(II) in the serum bottles were monitored by withdrawing 0.5 mL of suspension using N<sub>2</sub>-purged syringes, and were immediately acidified with 1 M HCl. After mixing vigorously, the acidified samples were centrifuged at 8,000 g for 10 min to remove particles and Fe(II) contents were determined with ferrozine at 562 nm. The dissolved fraction of Fe(II) was determined in the filtrates (0.2-µm cellulose acetate filter) acidified with 0.5 mL of 1 M HCl.

Samples for specific surface area analyses were measured using BET surface area analyzer (Micrometrics, ASAP 2020) using N<sub>2</sub> as the adsorbate. Single point surface area was determined following the standard procedure. For X-Ray Powder Diffraction (XRPD) analysis, powder samples were mounted on a glass sample holder using small amounts of grease. XRPD was performed using an X-ray diffractometer (XRD, Regaku D/max-II B) and a Cu Kα-radiation source (λ = 1.54056 Å) with 30 kV voltage and 20 mA current. The peak pattern for relevant iron oxides was compared with the standard peak pattern of pure iron oxide minerals available in the JCPDF database.

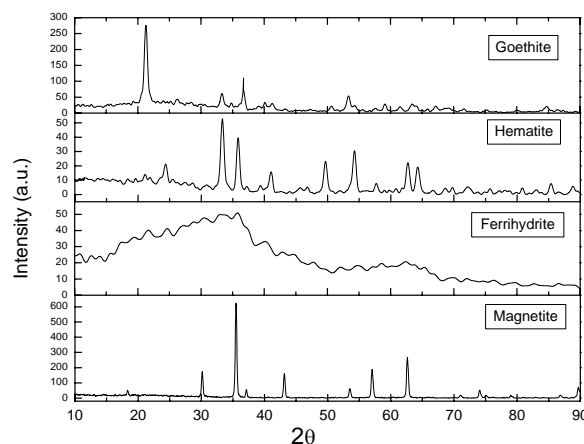


Fig. 1. The XRPD patterns of the synthesized iron oxide minerals.

## RESULTS AND DISCUSSION

### 1. Characterization of Iron Oxide Minerals

#### 1.1. Goethite

Figure 1 shows the XRPD patterns of synthesized iron oxide minerals. The bright yellow-colored iron oxide showed peaks at 21.22°, 36.72°, 33.34° and 53.24° 2θ with intensities of 100%, 26%, 18% and 17%, respectively, which is in good agreement with that of goethite in the JCPDF database. The needle shape of the synthesized mineral shown in the scanning electron microscopy (SEM) image is also a characteristic of goethite.

#### 1.2. Hematite

The iron oxide that was synthesized by the hematite preparation procedure had dominant peaks at 33.11°, 35.61°, 54.0° and 24.12° (2θ) with intensities of 100%, 70%, 36% and 24.12%, which are well-fitted with the XRD pattern of standard hematite in the JCPDF database. The SEM image indicates that the synthesized hematite is a well-crystallized fine particles with particle sizes of 30–50 nm, which is similar to that of the reported data.

#### 1.3. Magnetite

The XRPD patterns of the synthesized black colored minerals by using the procedure for the preparation of magnetite are shown in Fig. 1. The black color of the mineral provides preliminary evidence that the synthesized material could be magnetite. Moreover, the Cu Kα x-ray diffractogram shows dominant peaks at 35.42°, 62.51°, 30.09°, 56.94° and 43.05° (2θ) with intensity ratios of 100%, 40%, 30%, 30% and 20%, respectively, which can be assigned as magnetite. The cubic shapes with variable particle sizes in the range

50-200 nm were clearly observed in the SEM images.

#### 1.4. Ferrihydrite

In contrast to the other crystalline iron oxide minerals, ferrihydrite is a poorly crystalline mineral. Since XRPD only shows peaks for crystalline materials, the XRD pattern for ferrihydrite does not show any sharp peaks. As shown in Fig. 1, the synthesized ferrihydrite has two broad peaks at around 36.4° and 60.2°. This sort of ferrihydrite is referred to as two-line ferrihydrite.

#### 1.5. Specific surface area

The specific surface areas of iron oxides were determined by BET single point measurements using N<sub>2</sub> as an adsorbate. The determined values of specific surface areas were 28.80±0.11, 39.4±0.21, 222.00±0.30 and 11.67±0.08 m<sup>2</sup> g<sup>-1</sup> for goethite, hematite, ferrihydrite and magnetite, respectively.

### 2. Sorption of Fe(II) onto Iron Oxides

The sorption of heavy metal ions onto iron oxide minerals has been carried out by numerous studies with the objective of possible removal of metal ions from aqueous solutions [13]. However, only few studies focused on the sorption of Fe(II) species onto iron minerals, probably because Fe(II) ions are easily oxidized to Fe(III) in the presence of trace amounts of oxygen. Since sorbed Fe(II) ions on the Fe(III) oxides form Fe(II)/Fe(III) redox couple which often buffers the oxidation-reduction potential of anoxic systems, the sorption behavior of Fe(II) onto Fe(III) minerals may be compatible with the dechlorination behaviors of chlorinated hydrocarbons by surface-bound Fe(II) systems.

The Fe(II) adsorption on the goethite was studied at various concentration of Fe(II) ranging between 0.05 and 5 mM at 25 °C. The sorption of Fe(II) onto goethite followed Langmuir-type isotherm, which gives the relationship of the sorbed concentration on the surface of goethite and the equilibrium concentration:

$$\Gamma = \Gamma_{\max} \frac{K_{\text{ads}} [A]}{1 + K_{\text{ads}} [A]} \quad (1)$$

where  $\Gamma$  is the density of sorbate on the surface,  $\Gamma_{\max}$  is the maximum density of the sorbate,  $K_{\text{ads}}$  is the adsorption constant and  $[A]$  represents the aqueous concentration of adsorbate at equilibrium. As shown in Fig. 2, the sorption of Fe(II) on goethite can be well-fitted with Eq. 1, suggesting that Fe(II) sorption follows Langmuir isotherm. A previous study reported that the Fe(II) sorption on the goethite followed Lang-

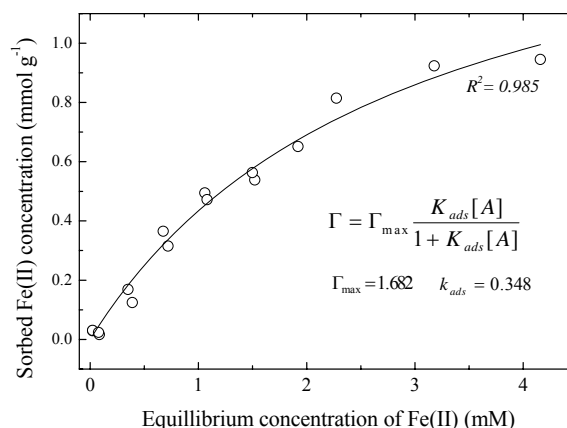


Fig. 2. The sorption isotherm of Fe(II) onto goethite at 25 °C.

Table 1. The sorption isotherms of Fe(II) onto various iron oxide minerals\*

Fe(III) oxide	Langmuir		Freundlich	
	$\Gamma_{\max}$	$K_{\text{ads}}$	K	1/n
Goethite	1.682	0.348	-	-
Hematite	1.231	0.899	-	-
Ferrihydrite	-	-	0.176	4.586
Magnetite	-	-	0.567	1.0

Note: \*The sorption of Fe(II) onto goethite and hematite followed Langmuir isotherm, while magnetite and ferrihydrite obeyed Freundlich isotherm.

muir isotherm at Fe(II) concentrations of 0-3 mM [14], which is consistent with the sorption isotherm of Fe(II) onto goethite obtained in this study.

The sorption isotherm of Fe(II) onto hematite also followed Langmuir isotherm (Table 1). The surface saturation level for hematite is lower than that for goethite, while the Fe(II)  $K_{\text{ads}}$  for hematite is larger. Ferrihydrite is a poorly crystalline Fe(III) mineral which has high specific surface area and exhibits amorphous characteristics. Therefore, ferrihydrite has been proven as an efficient sorbent for the removal of dissolved toxic metal ions. The sorption behavior of Fe(II) onto ferrihydrite is different from those in goethite and hematite systems. An exponential increase in sorbed Fe(II) density with increasing Fe(II) concentration in the solution was observed, which can be assigned as Freundlich isotherm. In addition, sorption of Fe(II) onto the magnetite was studied at the magnetite concentration of 2.32 g L<sup>-1</sup>. The sorption isotherm of Fe(II) onto magnetite also followed Freundlich isotherm with a good linearity, which the n value is almost equal to unity and the Freundlich constant (K) is 0.567.

### 3. Dechlorination of CT by Surface-bound Fe(II)

In order to compare the reductive capacities of

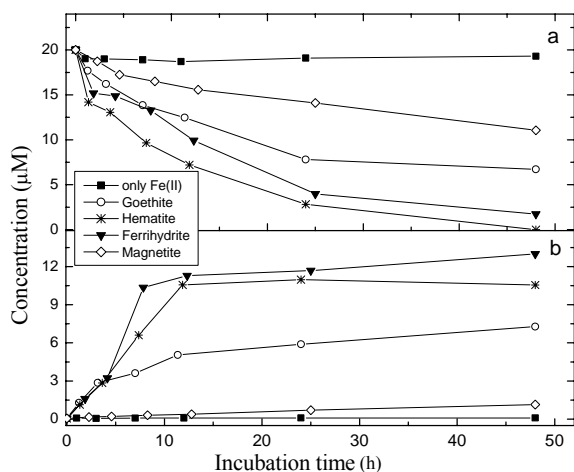


Fig. 3. Concentration profiles of dechlorination of CT by Fe(II) in the presence of various iron oxide minerals at pH 7.2 under anoxic conditions. (a) CT (b) CF.

dissolved and surface-bound Fe(II), CT was incubated with 3 mM Fe(II) at pH 7.2 in the absence and presence of iron oxide minerals. Figure 3a illustrates the dechlorination of 20 µM CT in Fe(II)-amended solution in the presence of iron oxides. No obvious change in CT concentration was observed during the experimental course in solutions containing Fe(II) alone. Several studies showed that CT can not be dechlorinated by dissolved Fe(II) at neutral pH during a relatively short time [14,15], which is consistent with the results obtained in this study. Addition of Fe(II) to the iron oxide suspensions increased the rate and efficiency of CT dechlorination. A nearly complete dechlorination of CT was observed within 48 h in the suspensions containing 10 mM hematite and 3 mM Fe(II). Nearly complete removal efficiencies of CT by Fe(II) were also observed in suspensions of ferrihydrite and goethite. However, the mixed-valence iron mineral, magnetite, showed a relative low reductive capacity and only 43% of the CT was dechlorinated within 48 h.

CF was found to be the major product in all the surface-bound Fe(II) systems (Fig. 3b). This result agrees with the previous observations that CT was dechlorinated by different types of Fe(II)/Fe(III) systems such as surface-bound Fe(II) associated with goethite and biogenic magnetite [16,17]. Because of the formation of CF, it is clear that reductive dechlorination is the prominent pathway for CT transformation. The maximum concentrations of CF in all the iron oxide systems except the magnetite system were in the range 7.3–13 µM. The production of CF concentration in magnetite system was only 1.14 µM. Table 2 shows the concentrations of CF after 48 h of incubation in surface-bound iron suspensions. It is clear that the mechanism for the reductive transformation of CT in each surface-bound system is not the same. The

Table 2. The percentage of CF to CT by surface-bound Fe(II) associated with different iron oxide system at pH 7.2

Iron oxide	$\Delta$ CT (µM)	Produced CF (µM)	[CF]/ $\Delta$ CT (%)
Goethite	12.68	7.28	57
Hematite	19.40	10.54	54
Ferrihydrite	17.68	12.99	74
Magnetite	8.35	1.14	14

carbon mass balance with respect to CF formation in surface-bound Fe(II) systems is 74% in ferrihydrite, 57% in goethite, 54% in hematite and 14% in magnetite systems, clearly showing that there may exist several degradation mechanisms for CT dechlorination. A trace amount of methane in the headspace was also detected by GC-MS in this study when a high concentration of CCl<sub>4</sub> (3 mM) was used in the dechlorination experiment, implying that further dechlorination to the less chlorinated byproducts or non-chlorinated final products occurred. Several studies showed that CCl<sub>4</sub> could be transformed to carbon monoxide and formate via reductive hydrolysis [16–18], suggesting that the loss of CCl<sub>4</sub> may be partially due to the formation of formate and carbon monoxide in the liquid phases.

The dechlorination of CT by the surface-bound Fe(II) species followed pseudo-first-order kinetics:

$$\ln \left[ \frac{C_t}{C_0} \right] = k_{obs} t \quad (2)$$

where  $C_0$  and  $C_t$  are the concentrations of CT at the initial and at time  $t$ , respectively, and  $k_{obs}$  is the observed pseudo-first-order rate constant. A good linear relationship between  $\ln(C_t/C_0)$  and time ( $t$ ) was observed during the first 10–20 h and then the slope decreased slightly. Such a deviation in the linearity has been reported to be a common phenomenon in the reduction of various compounds such as nitroaromatic compounds and polyhalogenated alkanes by surface-bound Fe(II) species [4,15,18]. The decrease in reactivity of surface-bound Fe(II) in the latter part of the experimental time is presumably attributed to the possible consumption of more reactive Fe(II) species at the first stage and the high affinity of surface reactive sites towards the produced compounds. Table 3 shows the  $k_{obs}$  values and the normalized surface area rate constant ( $k_{sa}$ ) for CT dechlorination in systems containing various types of iron oxides and 3 mM Fe(II) at pH 7.2. The  $k_{obs}$  for CT dechlorination followed the order: hematite > ferrihydrite > goethite > magnetite. When normalized to the specific surface area by dividing the  $k_{obs}$  by available surface area of iron oxide minerals in the serum bottles, the  $k_{sa}$  values followed the order: goethite ~ hematite > magnetite > ferrihydrite. Since similar molar concentration (10 mM) of iron oxides were amended into the bottles and the dechlorination in Fe(II)-Fe(III) suspension is a surface

Table 3. The rate constants for CT dechlorination by Fe(II) associated with various iron oxide minerals

Iron oxide	Surface area ( $\text{m}^2 \text{g}^{-1}$ )	Rate constants	
		$k_{\text{obs}}$ ( $\text{h}^{-1}$ )	$k_{\text{sa}}$ ( $\text{L h}^{-1} \text{m}^{-2}$ )
Goethite	28.8	0.0380	0.0296
Hematite	39.4	0.0836	0.0265
Ferrihydrite	222	0.0609	0.0051
Magnetite	11.7	0.0144	0.0106

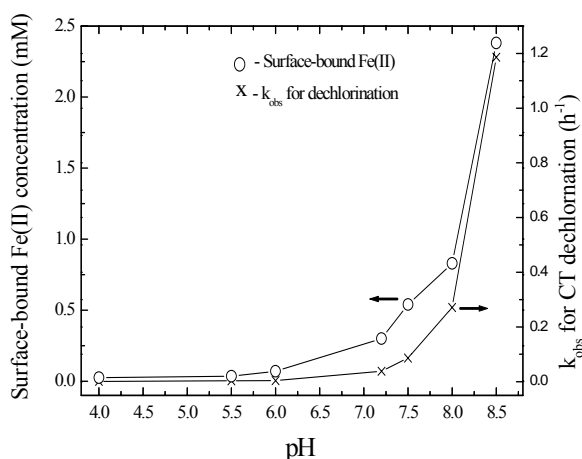


Fig. 4. The  $k_{\text{obs}}$  for CT dechlorination as a function of pH.

mediated reaction, it is reasonable to use  $k_{\text{sa}}$  to compare the dechlorination kinetics of CT in surface-bound Fe(II) associated with various iron oxides.

It is clear that goethite, the most abundant crystalline iron oxide, has the highest  $k_{\text{sa}}$  value, indicating the positive role in the abiotic dechlorination of chlorinated solvents. Hematite is also a well-crystalline and most stable iron oxide and has a high  $k_{\text{sa}}$  value. Magnetite is a relatively low stable crystalline mineral which bears structural Fe(II) and frequently generated by bacterial Fe(III) reduction. Its dechlorination capability with respect to  $k_{\text{sa}}$  is lower than those of goethite and hematite. Ferrihydrite, the amorphous iron mineral with high specific surface area, has the lowest  $k_{\text{sa}}$  value obtained in this study. This means that crystalline property of the iron mineral may be one of the important factors influencing the efficiency of CT dechlorination. Since goethite suspension has the highest capability for CT dechlorination, it is selected as the model iron oxide to examine the effect of pH on the dechlorination of CT in the subsequent experiments.

#### 4. Effect of pH on CT Dechlorination by Goethite

Figure 4 illustrates the effect of pH on  $k_{\text{obs}}$  for CT dechlorination in Fe(II)-goethite system. A 23% of the initial CT was dechlorinated after 350 h of incubation at pH 4, depicting that the reactivity of Fe(II)-goethite system is quite low at low pH. However, the dechlorination of CT increased up to 63% when the

pH increased to 6.5. The rapid increase in the dechlorination efficiency may be due to the change in pH from acid to neutral and then to basic. At pH 7.2, the CT concentration decreased from 20 to 6  $\mu\text{M}$  during 36 h of incubation. A nearly complete dechlorination of CT was occurred within 9 h when pH increased to 8.5. The  $k_{\text{obs}}$  values increased exponentially upon increasing pH values. A parallel series of serum boatels was prepared by following the similar procedures with the exception of CT amendments to determine the concentrations of surface-bound Fe(II). The surface-bound Fe(II) onto goethite surface also increased in the similar trend as the increase in the  $k_{\text{obs}}$ . This relationship clearly evidences that the increase in pH enhanced the rate and efficiency of CT dechlorination due to the increase in the surface-bound Fe(II) concentration.

### CONCLUSIONS

In this study, Fe(II) associated with iron oxides has demonstrated to be effective natural reductants for the dechlorination of chlorinated methanes. The reactivity of surface-bound Fe(II) species on the dechlorination is iron oxide-dependent. Comparison of the CT dechlorination by Fe(II) associated with iron oxides using  $k_{\text{sa}}$  shows that crystalline iron oxides are more reactive than amorphous ferrihydrite. Goethite has the highest reductive capability in dechlorinating chlorinated methanes, while ferrihydrite shows the lowest efficiency on CT dechlorination. The chlorinated product generated during reductive transformation of CT shows that the formation ratio of CF varies from 14% to 74%, which is dependent on the iron oxide minerals. The pH value is also an effective factor influencing the dechlorination of CT. Good removal efficiency of CT was observed at neutral and weakly alkaline pHs, depicting the positive impact on natural attenuation when using surface-bound iron species as the natural reductant. In the natural environments, the Fe(II)-Fe(III) reaction is one of the most important redox processes influencing the natural attenuation and in-situ remediation of priority pollutants in the subsurface environments. The Fe(II) ions can be generated from the reductive dissolution of ferric oxides by dissimilatory iron-reducing bacteria under anaerobic conditions. The generated Fe(II) can further sorb onto the surface of Fe(III) oxide, resulting in the formation of surface-bound iron species that can be used for long-term application to the remediation of groundwater contaminated with chlorinated hydrocarbons.

### ACKNOWLEDGMENTS

The authors thank National Science Council, Taiwan and University System of Taiwan for financial supports under contract No. NSC 92-2211-E-007-002 and 93J0334EJ, respectively.

## REFERENCES

1. Gillham, R.W. and S.F. O'Hannesin, Enhanced degradation of halogenated aliphatics by zerovalent iron. *Ground Water*, 32(6), 958-967 (1994).
2. Klausen, J., S.P. Tröber, S.B., Haderlein and R.P. Schwarzenbach, Reduction of substituted nitrobenzenes by Fe(II) in aqueous mineral suspensions. *Environ. Sci. Technol.*, 29(9), 2396-2404 (1995).
3. Haderlein, S.B. and K. Pecher, Pollutant reduction in heterogeneous Fe(II)-Fe(III) systems. In *Kinetics and Mechanisms of Reactions at the Mineral/Water Interface*. ACS Symposium Series, Division of Geochemistry, Sparks, D.L., Grundl, T.J., Eds., American Chemical Society: Washington, DC, Vol. 715, Chapter 17, pp. 342-357 (1998).
4. Elsner, M., R.P. Schwarzenbach and S.B. Haderlein, Reactivity of Fe(II)-bearing minerals toward reductive transformation of organic contaminants. *Environ. Sci. Technol.*, 38(3), 799-807 (2004).
5. Heijman, C.G., E. Grieder, C. Holliger and R.P. Schwarzenbach, Reduction of nitroaromatic compounds coupled to microbial iron reduction in laboratory aquifer columns. *Environ. Sci. Technol.*, 29(3), 775-783 (1995).
6. Kim, S. and F.W. Picardal, Enhanced anaerobic biotransformation of carbon tetrachloride in the presence of reduced iron oxides. *Environ. Toxicol. Chem.*, 18(10), 2142-2150 (1999).
7. Charlet, L., E. Silvester and E. Liger, N-compound reduction and actinide immobilization in surficial fluids by Fe(II): The surface  $\text{Fe}^{\text{III}}\text{OFe}^{\text{II}}\text{OH}^0$  species, as major reductant. *Chem. Geol.*, 151(1-4), 85-93 (1998).
8. Rügge, K., T.B. Hofstetter, S.B., Haderlein, P.L. Bjerg, S. Knudsen, C. Zraunig, H. Mosbaek and T. Christensen, Characterization of predominant reductants in an anaerobic leachate-contaminated aquifer by nitroaromatic probe compounds. *Environ. Sci. Technol.*, 32(1), 23-31 (1998).
9. Cepria, G., J.J. Cepria and J. Ramajo, Fast and simple electroanalytical identification of iron oxides in geological samples without sample pretreatment. *Microchim. Acta*, 144(1-3), 139-145 (2004).
10. Schwertman, U. and R.M. Cornell, *Iron Oxides in the Laboratory: Preparation and Characterization*. VCH Verlagsgesellschaft mbH. Weinheim D-6940, Germany, pp 61-79 (1991).
11. Maithreepala, R.A. and R.A. Doong, Reductive dechlorination of carbon tetrachloride in aqueous solutions containing ferrous and copper ions. *Environ. Sci. Technol.*, 38(24), 6676-6684 (2004).
12. Doong, R.A. and B. Schink, Cysteine-mediated reductive dissolution of poorly crystalline iron(III) oxides by *Geobacter sulfurreducens*. *Environ. Sci. Technol.*, 36(13), 2939-2945 (2002).
13. Venema, P., T. Hiemstra and W.H. van Eemsdijk, Multisite adsorption of cadmium on goethite. *J. Colloid Interface Sci.*, 183(2), 515-527 (1996).
14. Erbs, M., H.C.B. Hansen and C.E. Olsen, Reductive dechlorination of carbon tetrachloride using iron(II), iron(III) hydroxide sulfate (green rust). *Environ. Sci. Technol.*, 33(2), 307-311 (1999).
15. Amonette, J.E., D.J. Workman, D.W. Kennedy, J.S. Fruchter and Y.A. Gorby, Dechlorination of carbon tetrachloride by Fe(II) associated with goethite. *Environ. Sci. Technol.*, 34(21), 4606-4613 (2000).
16. McCormick, M.L. and P. Adriens, Carbon tetrachloride transformation on the surface of nanoscale biogenic magnetite particles. *Environ. Sci. Technol.*, 38(4), 1045-1053 (2004).
17. Maithreepala, R.A. and R.A. Doong, Synergistic effect of copper ion on the reductive dechlorination of carbon tetrachloride by surface-bound Fe(II) associated with goethite. *Environ. Sci. Technol.*, 38(1), 260-268 (2004).
18. Pecher, K., S.B. Haderlein and R.P. Schwarzenbach, Reduction of polyhalogenated methanes by surface-bound Fe(II) in aqueous suspensions of iron oxides. *Environ. Sci. Technol.*, 36(8), 1734-1741 (2002).

---

Discussions of this paper may appear in the discussion section of a future issue. All discussions should be submitted to the Editor-in-Chief within six months of publication.

**Manuscript Received: February 15, 2005**  
**Revision Received: November 15, 2005**  
**and Accepted: November 18, 2005**